A Study of the Photolysis and OH-initiated Oxidation of Acrolein and *trans*-Crotonaldehyde

I. Magneron, R. Thévenet, A. Mellouki,* and G. Le Bras

LCSR/CNRS, 1C Avenue de la Recherche Scientifique F-45071 Orléans Cedex 02- France

G. K. Moortgat

Max-Planck-Institut für Chemie, P.O. Box 3060, D-55020 Mainz, Germany

K. Wirtz

Fundation CEAM, Parque Tecnologico, E−46980 Paterna (Valencia), Spain

Received: September 5, 2001; In Final Form: November 19, 2001

Experiments have been conducted in the laboratory and in the outdoor smog chamber (EUPHORE) to study the photolysis and the OH-initiated oxidation of (1) acrolein (CH_2═CHCHO) and (2) *trans*-crotonaldehyde (CH_3CH═CHCHO). In addition, the UV−visible absorption spectra for these two unsaturated aldehydes have been determined at (298 ± 2) K, and the rate constants for OH reactions have been measured using PLP-LIF technique as function of pressure (20−300) Torr in the temperature range (243−372) K. The obtained rate constant values are $k_1 = (6.55 \pm 1.22) \cdot 10^{-12} \exp[(333 \pm 54)/T]$ and $k_2 = (5.77 \pm 1.14) \cdot 10^{-12} \exp[(533 \pm 58)/T]$ cm^3 molecule^{-1} s^{-1}. From both midday photolysis rates $J_1 \leq 2 \cdot 10^{-6}$ s^{-1} for acrolein and $J_2 \leq 1.2 \cdot 10^{-5}$ s^{-1} for *trans*-crotonaldehyde, measured at EUPHORE during summer, and UV−visible absorption cross sections, very low effective quantum yields were derived: $\Phi_{eff} \leq 0.005$ for acrolein, and $\Phi_{eff} \leq (0.030 \pm 0.006)$ for *trans*-crotonaldehyde. The major primary products of the OH-initiated oxidation were glyoxal and glycolaldehyde for acrolein and glyoxal and acetaldehyde for *trans*-crotonaldehyde. The obtained results indicate that at least 20% of the reaction of OH with acrolein proceeds by addition to the double bond. The atmospheric implications of the data are discussed. The major loss process is reaction with OH for the two aldehydes. Their atmospheric lifetimes are of few hours, and their impact mainly at a local scale will be the net HO_x (OH, HO_2) production through their photooxidation and that of the shorter chain carbonyl compounds produced.

Introduction

Carbonyl compounds are important precursors of radicals in the atmosphere. They are emitted as primary pollutants (from combustion, industrial uses, vegetation, and so on) or are produced as reaction intermediates from NO_x-mediated photooxidation of volatile organic compounds (VOCs) emitted into the atmosphere. It is well-established that the main degradation processes of carbonyl compounds in the gas phase are controlled by photolysis or reaction with OH, NO_3 radicals, and eventually with O_3 in the case of unsaturated compounds. As these processes can lead to the formation of additional radicals, they could be important with regard to the atmospheric oxidation capacity and local and regional formation of ozone and other photooxidants.

Acrolein (CH_2═CHCHO) and *trans*-crotonaldehyde (CH_3CH═CHCHO), on which this laboratory study is focused, are two unsaturated aldehydes emitted into the atmosphere through different sources such as combustion and chemical industries.[1] For example, acrolein is used in a number of agricultural chemicals and *trans*-crotonaldehyde can be found in at least two industrial sectors (cellulosic manmade fibers and industrial organic chemicals).[2] In addition, acrolein and *trans*-crotonaldehyde are both released to the atmosphere from the combustion of wood, polymers, tobacco, and gasoline. Acrolein is also a product of the atmospheric OH- and O_3-initiated oxidation of 1,3 dienes.[3] In several large cities, ambient concentrations up to 9 ppb of acrolein have been reported.[4] Similarly to other unsaturated carbonyl compounds, the atmospheric fate of acrolein and *trans*-crotonaldehyde can be controlled in the gas phase by photolysis, reactions with OH, NO_3 radicals, and O_3. The available kinetic data indicates that reactions with NO_3 radicals[5,6] and O_3[7−10] are less important than that with OH radicals under typical atmospheric conditions. The contribution of the photolysis is not well established because of the lack of data for atmospheric conditions.

The existing data for the OH reaction rate constants with acrolein and *trans*-crotonaldehyde were all obtained at room temperature using the relative-rate technique.[11−14] The four reported rate constants for OH reaction with acrolein are in the range $(1.83-2.66) \cdot 10^{-11}$ cm^3 molecule^{-1} s^{-1} and can be considered in agreement. The two values reported so far for the OH reaction rate constant with *trans*-crotonaldehyde are in good agreement: $(3.3 \pm 0.6) \cdot 10^{-11}$ and $(3.5 \pm 0.4) \cdot 10^{-11}$ cm^3 molecule^{-1} s^{-1}.[11,13] The photolysis of the two aldehydes has been subject of a few studies, but the available quantum yield data for the different photolysis channels remain uncertain, and the photolysis rates in atmospheric conditions are still unknown.[15−17] Only one product study on the OH-initiated oxidation of acrolein has been published so far.[18]

The objectives of this work were to investigate the atmospheric degradation of acrolein and *trans*-crotonaldehyde to assess the importance of different gas-phase processes. In this

* Corresponding author: mellouki@cnrs-orleans.fr.

10.1021/jp013413a CCC: $22.00
Published on Web 02/19/2002

respect, the OH reaction rate constants with these two aldehydes were measured as function of pressure (20−300 Torr) and temperature (243−372 K), using the pulsed laser photolysis−laser induced fluorescence technique. In addition, the OH-initiated oxidation mechanisms were investigated in the laboratory and in a large outdoor simulation chamber facility, EUPHORE (EUropean PHOto REactor). Finally, the UV−visible absorption spectra and the photolysis rates were measured, and the products were determined under different conditions for both compounds. The experiments were performed in different laboratories (LCSR/CNRS−Orléans, MPI-Mainz, and EUPHORE-Valencia). The obtained data enable us to have a better understanding of the atmospheric fate of acrolein and *trans*-crotonaldehyde.

Experimental Section

The experimental systems and the procedures used in different laboratories are briefly described here, more details can be found elsewhere.[19−22]

OH Reactions Rate Constant Measurements. The pulsed laser photolysis−laser induced fluorescence (PLP−LIF) technique was used at CNRS/LCSR−Orléans to measure the absolute rate constants of the OH reaction with the two unsaturated aldehydes. OH radicals were produced by photolysis of H_2O_2 at $\lambda = 248$ nm (KrF excimer laser). The OH temporal concentration profiles were obtained by pulsed laser-induced fluorescence using a Nd:YAG pumped frequency-doubled dye laser, which was triggered at a variable delay time after the photolysis pulse. The probe pulse excited OH at $\lambda \approx 282$ nm, and its fluorescence was collected at around 309 nm.

The reactions were studied under pseudo-first-order conditions in OH radical concentrations: $[\text{aldehyde}]_o \gg 100[\text{OH}]_o$ with $[\text{OH}]_o < 2 \cdot 10^{11}$ molecule cm^{-3}. Under these conditions, the OH concentration time profiles followed the pseudo-first-order rate law:

$$[\text{OH}]_t = [\text{OH}]_o e^{-k't} \text{ where } k' = \text{k}[\text{aldehyde}] + \text{k}'_o$$

k is the rate coefficient for the reaction of OH with the aldehyde and the decay rate, k'_o, is the first-order OH decay rate in the absence of the aldehyde. The value of k'_o is essentially the sum of the reaction rate of OH with its precursor (H_2O_2) and the diffusion rate of OH out of the detection zone. Helium was used as the bath gas.

OH-Initiated Oxidation Investigation. The OH-initiated oxidation of acrolein and *trans*-crotonaldehyde was investigated at CNRS/LCSR in Orléans and at the EUPHORE outdoor simulation chambers.

(i) Experiments Performed at CNRS−Orléans. The setup used at Orléans consists of a FEP Teflon bag with a volume of about 140 L surrounded by 6 lamps emitting at 254 nm (Sylviana, G 30W) and 6 lamps emitting between 300 and 460 nm, centered on 365 nm (Philips, TL 20W/05). The bag and the lamps were positioned in a wooden box with internal faces covered with aluminum foil. The number of lamps could be selected to vary the total intensity of light. Air was flowed to stabilize the temperature at 298 ± 3 K. The carbonyl compounds were introduced in the bag through a stream of purified air by flushing a known amount from calibrated bulbs. The photoreactor was then filled to its full capacity at atmospheric pressure with purified air. Analysis was performed using a Nicolet FTIR spectrometer with a path-length of 10 m. Infrared spectra were taken at 1 cm^{-1} resolution. The initial concentrations were in the range 50−120 and 80−130 ppm for acrolein and *trans*-crotonaldehyde, respectively. OH radicals were produced from the photolysis of HONO or H_2O_2 using the lamps centered at 365 or 254 nm, respectively. Typically, the homogenized reaction mixture was irradiated for a duration of 50−150 min.

(ii) Experiments Performed at EUPHORE. A detailed description of the EUPHORE facility and the existing analytical equipment can be found elsewhere;[21,22] however, a brief description is given here. The EUPHORE facility consists of two independent hemispherical outdoor simulation chambers, made of fluorine−ethene−propene (FEP) foil, with a volume of 200 m^3 each. The used FEP foil has more than 80% transmission of the solar radiation in the wavelength range between 290 and 520 nm. Both chambers are equipped with FTIR spectrometers coupled with White-type multipath mirror systems for in situ analysis. The optical path lengths were 326.8 m in one chamber and 553.5 m in the other one. The IR spectra were recorded every 10 min by co-adding 550 interferograms with a resolution of 1 cm^{-1}. Analysis was also accomplished using gas chromatographs equipped with different detectors (flame ionization (FID), photoionization (PID), and electron capture (ECD)). O_3, CO, and NO_x were analyzed using specific analyzers, Monitor Labs 9810, Thermo Environment 48C, Monitor Labs 9841A and ECO−Physics CLD770 AL ppt with PLC 760 photolytic converter, respectively. Reactant and product concentrations were determined using calibrated reference spectra. Known amounts of reactants (acrolein or *trans*-crotonaldehyde) were introduced into the chambers at the ppm level along with SF_6 used to measure the dilution rate caused by minor leaks, the thermal expansion of the reaction mixture, and the sampling of the connected instruments. In the photolysis experiments, cyclohexane or di-*n*-butyl ether were also added to scavenge OH radicals or to estimate their concentration (see Results and Discussion). During the OH-initiated oxidation experiments, NO was added to initiate the OH radical formation under sunlight conditions. The actinic flux was measured by using a calibrated filter radiometer specific to the photolysis frequency of NO_2. For each experiment, the analysis of the gas mixture was started for at least 30 min before exposing the mixture to the sunlight to check for any dark effect.

UV Absorption Cross Sections Measurements. The room-temperature UV−visible absorption spectra of acrolein and *trans*-crotonaldehyde were determined at MPI-Mainz and LCSR/CNRS−Orléans.

(i) Experiments Performed at MPI-Mainz. The cross sections were measured in a 63 cm long, triple-jacketed quartz cell (i.d. 3 cm). Transmitted light from a deuterium lamp through a Jobin Yvon monochromator (HRS 2) was detected with a 1024 pixel diode array detector (InstaSpecII, Oriel). Measurements were performed over the wavelength region $\lambda = 220-400$ nm. Absorption cross sections were obtained using the Beer−Lambert law:

$$\sigma(\lambda) = -\ln[I(\lambda)/I_o(\lambda)]/LC$$

where I and I_o are the light intensities for the filled and empty cell, respectively, L is the length of the absorption cell, and C is the concentration of the compound in the cell. The spectrometer recorded spectra over about 70 nm (600 grooves/mm, resolution of 0.3 nm), and the wavelength scale was calibrated using lines from Zn (213.8 nm) and Hg Penray lamps (253.65, 296.73, and 365.02 nm). The measurements were performed in static conditions, in a pressure range of 0.02−10 Torr, at room temperature (298 ± 3 K). The pressure was measured with 0−10

and 0−1000 Torr capacitance manometers, and the final spectrum in each range was the average of three or four similar spectra.

(ii) Experiments Performed at CNRS−Orléans. The collimated output of a deuterium lamp (Oriel 30 W) passed through an absorption cell and was focused onto the entrance slit of a spectrograph equipped with a 1800 grooves/mm grating, which dispersed the radiation onto a 1024 element diode array detector (Chromex 250IS, Princeton Instrument, Inc.). The absorption cell, equipped with quartz windows, was made of Pyrex and was 100 cm long with an internal diameter of 2.5 cm. Measurements were made over the wavelength region 230−390 nm; the wavelength scale was calibrated using the same lines as those used at MPI. The Beer−Lambert law was used to derive the absorption cross sections, σ. The measurements were performed over 40 nm, at (298 ± 2) K, in static conditions in the pressure range 2−30 Torr. The pressure was measured with 0−10 and 0−1000 Torr capacitance manometers, and the final spectrum in each range was the average of three or four similar spectra.

Photolysis Investigation. Photolysis experiments of acrolein and *trans*-crotonaldehyde were conducted at room temperature under different conditions using (i) a quartz cell in the laboratory at MPI-Mainz and (ii) the EUPHORE outdoor smog chamber.

(i) Experiments Performed at MPI-Mainz. The experiments were performed in a 44.2 L (1.40 m length and 20 cm diameter) quartz cell, equipped with two independent sets of White-optic mirror arrangements. One of them consists of sapphire-coated aluminum mirrors and was used for infrared measurements. The other set of mirrors consisted of MgF_2-coated aluminum and was used for UV−visible absorption measurements. The base distance between the mirrors was 1.2 m. In these experiments, the IR path was tuned at 28 passes (33.6 m) and the UV path at 8 passes (9.82 m). Photolysis was achieved by using TL12 sunlamps (275−380 nm, maximum at 310 nm, Philips 40W), radially mounted around the cell.

A FTIR spectrometer (Bomem DA8) was used to measure the concentrations of aldehydes and their photolysis products. Infrared spectra were taken at 0.5 cm^{-1} resolution in the range of 450−4000 cm^{-1}. Concentration−time profiles were measured every 5 min at the beginning of the experiment and every 10 min after about 30 min photolysis time. The experiments were carried out in synthetic air at various total pressures (100−700 Torr) and at 296 ± 2 K. The typical aldehyde initial concentrations were in the range of 12−150 ppm. Qualitative and quantitative data evaluations were carried out by comparing the product spectra with reference ones obtained in the same cell and using calibration curves at corresponding pressures and resolution. It has to be noted that the photolysis rates measured in these conditions correspond to lamps used.

(ii) Experiments Performed at EUPHORE. Known amounts of reactants were introduced to the chamber in a stream of dry air. The experiments were performed in the presence of SF_6, to derive the dilution rate. This dilution rate (k_{SF6}) is given by:

$$\ln([SF_6]_0/[SF_6]_t) = k_{SF6}t$$

where $[SF_6]_0$ and $[SF_6]_t$ are the initial SF_6 concentration and after reaction time t, respectively. Photolysis experiments in air have been conducted in the presence of OH tracer (di-*n*-butyl ether) or scavenger (cyclohexane) in order to estimate or scavenge the residual OH in the chamber. In these conditions, the aldehyde (acrolein or *trans*-crotonaldehyde) is lost by photolysis, by reaction with OH in the absence of the scavenger (in the presence of tracer), and by dilution. The disappearance of di-*n*-butyl ether is only due to its dilution in the chamber and to its reaction with OH radicals:

$$\text{aldehyde} + h\nu \rightarrow \text{products} \quad J$$

$$\text{aldehyde} + \text{OH} \rightarrow \text{products} \quad k_{OH}$$

$$\text{aldehyde} \rightarrow \text{loss by dilution} \quad k_{SF6}$$

$$\text{di-}n\text{-butyl ether} + \text{OH} \rightarrow \text{products} \quad k_{DNBE}$$

$$\text{di-}n\text{-butyl ether} \rightarrow \text{loss by dilution} \quad k_{SF6}$$

It can be shown that:

$$\ln([\text{aldehyde}]_0/[\text{aldehyde}]_t) = (J + k_{OH}[OH] + k_{SF6})t = k_{total}t$$

under the assumption that the OH radical concentration remains constant during the photolysis experiment.

The presence of an excess cyclohexane prevents the contribution of OH reaction to the consumption of the studied aldehydes and to the chemistry of the observed products ($[\text{cyclohexane}]_0 > 30 \times [\text{aldehyde}]_0$). The excess of cyclohexane suppresses the term $k_{OH}[OH]$ in the above equation. On the other hand, the use of the tracer, di-*n*-butyl ether, enables estimation of the OH concentration in the chamber during the photolysis experiments. This OH concentration is derived from the first-order decay of the tracer concentration, and it is then used to estimate the contribution of the OH reaction to the loss of the studied aldehyde. The OH concentration, [OH], is then given by:

$$\ln([DNBE]_0/[DNBE]_t) = (k_{DNBE}[OH] + k_{SF6})t = k_{tracer}t$$

k_{SF6} was measured during each run while $k_{DNBE} = 2.96 \cdot 10^{-11}$ cm^3 $molecule^{-1}$ s^{-1}.[23]

Material. *trans*-crotonaldehyde and acrolein were obtained from Fluka with purities, respectively of >99.5% and >95%. Before use, all samples were degassed by several freeze−pump−thaw cycles.

Results and Discussion

OH Rate Constant Measurements. Examples of plots of ($k' - k'_o$) versus acrolein and *trans*-crotonaldehyde concentrations obtained at room temperature are shown in Figure 1. The reaction rate constants k_1 and k_2

$$CH_2{=}CHCHO + \text{OH} \rightarrow \text{products} \quad k_1$$

$$CH_3CH{=}CHCHO + \text{OH} \rightarrow \text{products} \quad k_2$$

were derived from the least-squares fit of the straight lines. The quoted errors for the determined rate constants include 2σ from the least-squares analysis and an estimated systematic error of 5%. The summary of the experimental conditions and the obtained rate constants are given in Tables 1 and 2. The change in the fluence of the laser photolysis did not have any influence on the obtained data. Most experiments were conducted at around 100 Torr. However, experiments performed between 20 and 300 Torr showed that the total pressure had no effect on the obtained rate constants. The absence of pressure dependence of k_1 and k_2, in the range of this study (20−300 Torr), indicates that the high-pressure limit is already reached at $P = 20$ Torr of helium. The average values at 298 K are $k_1 = (1.99 \pm 0.24) \cdot 10^{-11}$ and $k_2 = (3.35 \pm 0.30) \cdot 10^{-11}$ cm^3 $molecule^{-1}$ s^{-1}.

TABLE 1: Reaction of acrolein with OH: Experimental Conditions and Measured Rate Constant in the Temperature Range 243−372 K

T (K)	P (Torr)	[acrolein] (10^{13} molecule cm^{-3})	k'_o (s^{-1})	k (s^{-1})	$(k \pm 2\sigma) \cdot 10^{11}$ (cm^3 molecule^{-1} s^{-1})[a]
243	100	2.49−31.1	220−261	1110−8680	2.66 ± 0.04
253	100	2.37−30.16	194−256	1018−7948	2.53 ± 0.09
273	100	2.25−34.91	140−217	853−8005	2.25 ± 0.06
273	100	1.69−21.02	115−189	565−4737	2.19 ± 0.04
273	50	3.36−59.86	178−304	1275−14548	2.33 ± 0.10
273	30	2.02−42.98	273−345	951−10162	2.27 ± 0.04
298	300	2.17−45.27	175−252	886−9485	2.02 ± 0.04
298	100	2.01−39.00	142−202	761−8198	2.03 ± 0.03
298	100	2.12−25.53	160−191	783−5574	2.07 ± 0.06
298	100	1.86−30.10	167−232	677−6428	2.04 ± 0.05
298	100	1.81−18.89	116−160	523−3679	1.86 ± 0.04
298	100	1.75−19.57	115−159	522−3969	1.96 ± 0.04
298	50	1.97−31.09	192−292	791−6670	2.06 ± 0.08
298	20	1.38−30.44	330−365	785−6767	2.07 ± 0.06
323	100	2.93−24.53	123−179	649−4748	1.88 ± 0.10
323	100	1.58−18.11	129−157	458−3400	1.80 ± 0.04
348	100	1.99−21.79	135−168	613−4145	1.80 ± 0.05
372	100	1.67−25.01	156−175	551−4379	1.68 ± 0.03

[a] Uncertainties are the 2σ precision of the least-squares fits of $k' - k'_o$ vs [acrolein].

TABLE 2: Reaction of *trans*-crotonaldehyde with OH: Experimental Conditions and Measured Rate Constant in the Temperature Range 243−372 K

T (K)	P (Torr)	[*trans*-crotonaldehyde] (10^{13} molecule cm^{-3})	k'_o (s^{-1})	k' (s^{-1})	$(k \pm 2\sigma) \cdot 10^{11}$ (cm^3 molecule^{-1} s^{-1})[a]
243	100	0.49−5.51	106−155	344−3033	5.30 ± 0.11
253	100	0.85−8.43	96−145	517−4071	4.88 ± 0.19
273	100	0.63−11.32	156−211	589−4731	3.98 ± 0.09
273	30	1.05−22.50	237−329	869−8457	3.59 ± 0.11
273	20	0.30−15.34	357−400	638−5860	3.66 ± 0.13
298	300	1.49−13.28	154−189	642−4644	3.49 ± 0.18
298	100	0.76−9.25	107−146	392−3254	3.47 ± 0.17
298	100	0.65−21.02	136−230	517−7193	3.22 ± 0.10
298	100	0.48−20.76	152−205	501−7192	3.32 ± 0.12
298	100	0.89−6.98	167−190	492−2506	3.40 ± 0.14
298	50	1.5−6.21	162−207	757−2559	3.74 ± 0.07
298	30	1.0−7.94	222−291	626−3029	3.64 ± 0.18
298	20	0.62−4.77	277−305	597−2029	3.63 ± 0.25
323	105	0.31−7.42	122−191	388−5624	3.06 ± 0.14
348	100	2.41−7.47	133−173	909−4763	2.64 ± 0.08
372	100	0.94−12.78	151−171	493−3356	2.52 ± 0.13

[a] Uncertainties are the 2σ precision of the least-squares fits of $k'_- - k'_o$ vs [*trans*-crotonaldehyde].

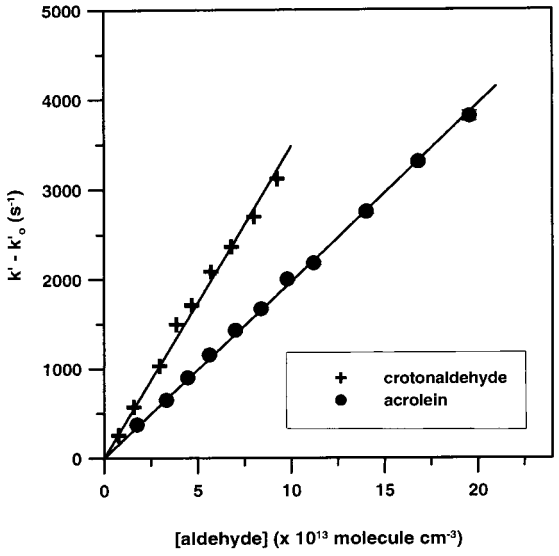

Figure 1. Reaction of acrolein and *trans*-crotonaldehyde with OH. Pseudo-first-order plots at 298 K and 100 Torr.

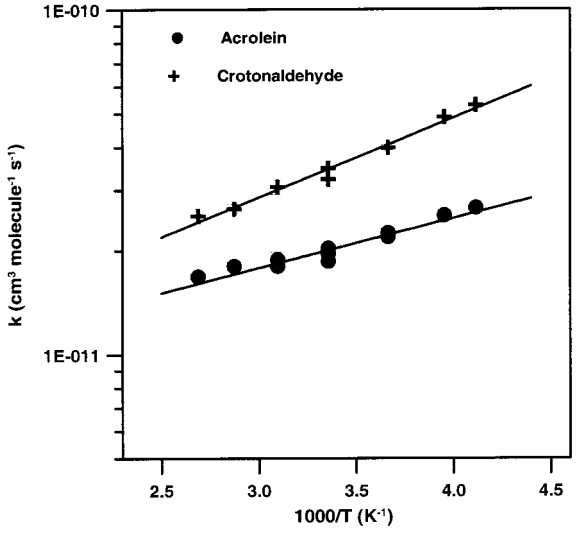

Figure 2. Arrhenius plots of reaction rate constants of acrolein and trans-crotonaldehyde with OH at 100 Torr.

The measured rate coefficients for the reactions of OH with the two unsaturated aldehydes determined over the temperature range 243−372 K are shown in Figure 2 in the conventional Arrhenius form ($k = Ae^{-Ea/RT}$). They are well represented by

TABLE 3: Summary of the Available Rate Constant Data for the Reaction of Acrolein and *trans*-Crotonaldehyde with OH at 298 ± K

compound	$(k \pm 2\sigma)$ $(10^{-11})^a$	A $(10^{-12})^a$	E/R (K)	technique[b]	reference
acrolein CH_2═CHCHO	2.66 ± 0.33^c			RR	11
	1.90 ± 0.20^d			RR	12
	1.83 ± 0.13^e			RR	13
	2.04 ± 0.01^f			RR	14
	1.99 ± 0.24	6.55 ± 1.22	333 ± 54	PLP-LIF	this work
trans-crotonaldehyde CH_3CH═CHCHO	3.30 ± 0.60^d			RR	12
	3.50 ± 0.40^e			RR	13
	3.35 ± 0.30	5.77 ± 1.14	533 ± 58	PLPFIL	this work

[a] In cm^3 $molecule^{-1}$ s^{-1}. [b] RR = relative rate technique; PLP-LIF = pulsed laser photolysis−laser induced fluorescence. [c−f] The reference compounds were (c) butane ($k = 2.66 \cdot 10^{-11}$), (d) ethene ($k = 8 \cdot 10^{-12}$), (e) propene ($k = 2.52 \cdot 10^{-11}$), and (f): propene ($k = 2.65 \cdot 10^{-11}$) (with values of k in cm^3 $molecule^{-1}$ s^{-1}).

the following expressions (in cm^3 $molecule^{-1}$ s^{-1}):

$$k_1 = (6.55 \pm 1.22) \cdot 10^{-12} \exp[(333 \pm 54)/T]$$

$$k_2 = (5.77 \pm 1.14) \cdot 10^{-12} \exp[(533 \pm 58)/T]$$

where the quoted errors are $\Delta A = 2A\sigma_{\ln A}$ and $\Delta E/R = 2\sigma_{E/R}$. The plots show a negative temperature dependence of the rate constants for both aldehydes. The Arrhenius parameters for the OH reactions with these aldehydes are given in Table 3, where the obtained data are summarized along with those from previous studies. As observed from this table, our values at room temperature are in agreement with those reported previously by different groups using the relative-rate method.[11−14] We report here the first absolute measurements as well as the first temperature-dependence studies of these two reactions.

The two reactions are expected to proceed by addition to the double bond or by H-atom abstraction of the aldehydic hydrogen and in the case of *trans*-crotonaldehyde also from the methyl group. The observed negative temperature dependence of both rate constants, k_1 and k_2, may not be explained only by an addition mechanism. Such temperature dependence has been also observed, in the same temperature range of this study, for reactions of OH radicals with simple aldehydes such as propanaldehyde, *n*-butyraldehyde, *n*-pentaldehyde, *iso*-butyraldehyde, and *tert*-butyraldehyde.[24,25] This was attributed to a possible reaction proceeding through a direct H-atom abstraction or through addition−elimination with formation of a long-lived intermediate.[24,26] However, it is expected that both addition of OH to the double bond and net H-atom abstraction from −CHO occur, as it was reported for the OH-initiated oxidation of methacrolein (CH_2═$C(CH_3)$CHO) which has a structure comparable to those of acrolein and *trans*-crotonaldehyde.[27,28]

We have applied the structure−activity relationship (SAR) of Atkinson[29] to estimate the contribution of each site to the overall reactions of OH with the two unsaturated aldehydes. In this method, calculation of H-atom abstraction for C−H bonds is based on the estimation of $-CH_3$, $-CH_2-$, and −CH< group rate constants, assuming that they depend on the identity of substituents attached to the groups. At 298 K, the group rate constants are given by

$$k(CH_3-X) = k_{prim}F(X)$$

$$k(Y-CH_2-X) = k_{sec}F(X)F(Y)$$

$$k((Y)(Z)CH(X)) = k_{tert}F(X)F(Y)F(Z)$$

where k_{prim}, k_{sec}, k_{tert} are the rate constants per $-CH_3$, $-CH_2-$, >CH− groups and $F(X)$, $F(Y)$, $F(Z)$ are the substituent factors. For the compounds with alkene groups, the contribution of the addition rate constant to the overall rate constant can also be estimated and depends on the nature of the substituent groups. Therefore, the estimation of the rate constants of OH with acrolein and *trans*-crotonaldehyde are given, respectively by

$$k_1 = k(CH_2{=}CH) \cdot C(CHO) + k_{tert} \cdot F(=O) \cdot F(CH_2{=}CH)$$

$$k_2 = k_{prim} \cdot F(CH{=}CH) + k(CH{=}CH) \cdot C(CHO) \cdot C(CH_3) + k_{tert} \cdot F(=O) \cdot F(CH{=}CH)$$

Using the following previously published parameters,[29] $k_{prim} = 0.136 \cdot 10^{-12}$, $k_{tert} = 1.94 \cdot 10^{-12}$, $k(CH_2{=}CH) = 26.3 \cdot 10^{-12}$, and $k(CH{=}CH) = 64 \cdot 10^{-12}$ (in units of cm^3 $molecule^{-1}$ s^{-1}), $F(=O) = 8.7$, $F(CH_2{=}CH) = F(CH{=}CH) = 1$, $C(CHO) = 0.34$, and $C(CH_3) = 1$, we found that the experimental and calculated values k_1 and k_2 are in fair agreement (the calculated values are in parentheses): $k_1 = 2.0 \pm 0.2$ (2.6) and $k_2 = 3.4 \pm 0.3$ (3.9) (in units of 10^{-11} cm^3 $molecule^{-1}s^{-1}$).

The use of Atkinson's SAR indicates that the reaction of OH with acrolein proceeds mainly by H-atom abstraction from the −CHO group (65%) and the addition to the double bond represents about 35%. The addition of OH to the double bond of *trans*-crotonaldehyde seems to be slightly more important than the H-atom abstraction from the −CHO group, 56% and 44%, respectively. The contribution of the methyl group in this latter molecule is calculated to be negligible (0.4%). We have undertaken an experimental mechanistic study of the OH-initiated oxidation of the two aldehydes in order to evaluate the importance of each reaction pathway and compare it with the SAR estimation.

OH-Initiated Oxidation Investigation. Experiments were conducted using a small Teflon bag at LCSR/CNRS−Orléans and under natural sunlight conditions using the large-volume chambers at the EUPHORE facility. Calibration of the IR spectra of the reactants and the products involved in this study were conducted in the laboratory or at EUPHORE.

(i) Acrolein. **(a) Laboratory Studies.** The initial acrolein and NO concentration ranges were 53−118 and 8−15 ppm, respectively. 50−90% of the acrolein introduced in the chamber were consumed during the experiments corresponding to a reaction time typically in the range 50−120 min. Analysis were performed by using FTIR. Figure 3 shows an example of typical IR spectra of the gas mixture recorded before and after 90 min of irradiation. Glyoxal (CHOCHO), glycolaldehyde ($HOCH_2CHO$), and ketene (H_2CCO) were observed as primary reaction products with initial yields of (5 ± 2)%, (25 ± 10)%, and (3 ± 2)%, respectively. The other observed products were formaldehyde (HCHO), CO, and formic acid (HCOOH); their

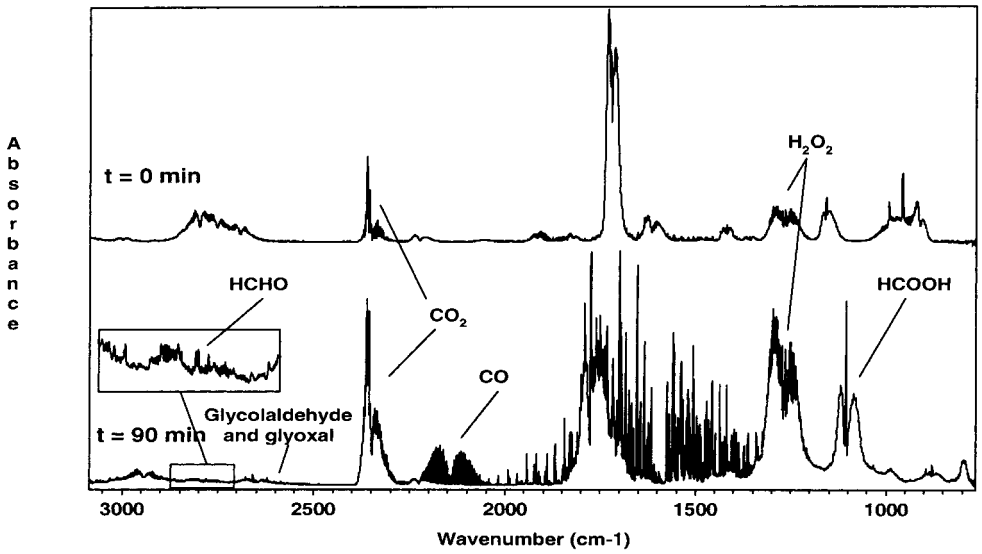

Figure 3. OH-initiated oxidation of acrolein, FTIR spectra before (t = 0 min) and after irradiation (t = 90 min) (data from the laboratory).

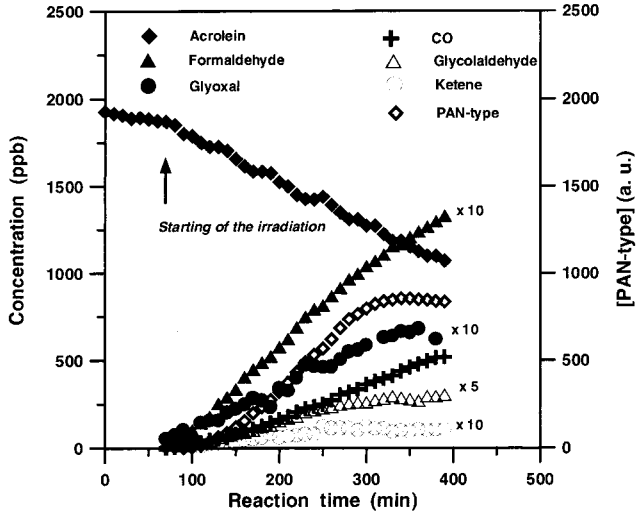

Figure 4. OH-initiated oxidation of acrolein, experimental concentration profiles of the reactant and products (at EUPHORE).

concentration−time profiles indicated that they were essentially secondary products of the reaction although CO may also be partly a primary product; hence, no yields could be derived. The carbon balance at the end of the experiment was estimated to be around 76%. The concentration−time profiles of the reactant and products were obtained from integration of the IR spectra between 1650 and 1780 cm^{-1} for acrolein, 2700−2970 cm^{-1} for glycolaldehyde, 2725−2935 cm^{-1} for glyoxal, 2640−3080 cm^{-1} for formaldehyde, 2020−2230 cm^{-1} for CO, 1035−1170 cm^{-1} for formic acid, and 2060−2230 cm^{-1} for ketene.

(b) EUPHORE Studies. A single experiment was performed in the presence of 1.9 ppm of acrolein, 80 ppb of NO, and 60 ppb of NO_2. The mixture was exposed to natural sunlight for 6 h. As it can be seen from Figure 4, the obtained concentration time profiles of the reactants and products confirm the observation of the laboratory. Formaldehyde, glyoxal, glycolaldehyde, CO, formic acid, and ketene were observed as products. In addition, a PAN-type compound, probably $CH_2{=}CHC(O)O_2NO_2$, was detected by GC−ECD but could not be quantified in the absence of a calibrated reference sample. Similarly to the results obtained in the laboratory, the products yields were derived for the primary products glyoxal, glycolaldehyde, and ketene to be 10%, 13%, and 2%, respectively.

The observed products in both experiments can be explained by a mechanism proceeding by both H-atom abstraction of the aldehydic hydrogen and OH-addition to the carbon−carbon double bond. The abstraction from the −CHO group channel may lead to $CH_2{=}CHC(O)O_2NO_2$ through

$$CH_2{=}CHCHO + OH \rightarrow CH_2{=}CHCO + H_2O$$

$$CH_2{=}CHCO\ (+O_2\ +M) \rightarrow CH_2{=}CHC(O)O_2$$

$$CH_2{=}CHC(O)O_2 + NO_2\ (+M) \rightarrow CH_2{=}CHC(O)O_2NO_2$$

The $CH_2{=}CHC(O)O_2$ radical may also react with NO depending on the ratio $[NO_2]/[NO]$ during the experiment:

$$CH_2{=}CHC(O)O_2 + NO \rightarrow CH_2{=}CHC(O)O + NO_2$$

$$CH_2{=}CHC(O)O\ (+M) \rightarrow CH_2{=}CH + CO_2$$

$$CH_2{=}CH + O_2\ (+M) \rightarrow CH_2{=}CHO_2$$

$$CH_2{=}CHO_2 + NO \rightarrow CH_2{=}CHO + NO_2$$

The vinoxy radical, $CH_2{=}CHO$, reacts with O_2 to form ketene, glyoxal, and formaldehyde.[30,31] The following reaction channels have been suggested:

$$CH_2{=}CHO + O_2\ (+M) \rightarrow [OOCH_2{=}CHO]$$

$$[OOCH_2{=}CHO] \rightarrow CHOCHO + OH$$

$$[OOCH_2{=}CHO_2] \rightarrow HCHO + CO + OH$$

alternatively,

$$CH_2{=}CHO \leftrightarrow HOCH{=}CH$$

$$HOCH{=}CH + O_2\ (+M) \rightarrow HOCH_2{=}CHO_2$$

$$HOCH_2{=}CHO_2 \rightarrow HCO + HCOOH$$

$$HCO + O_2 \rightarrow HO_2 + CO$$

The decomposition of $CH_2{=}CHC(O)$ radical produced in the first step of the reaction, resulting from the OH abstraction of

the aldehydic hydrogen, is not excluded:[32]

$$CH_2{=}CHC(O)\ (+M) \rightarrow CH_2{=}CH + CO$$

On the other hand, the addition of OH to the carbon−carbon double bond followed by reaction with O_2/NO produces two different β-hydroxy alkoxy radicals:

$$CH_2{=}CHCHO + OH\ (+ O_2/NO, + M) \rightarrow HOCH_2CH(O)CHO + NO_2$$

$$CH_2{=}CHCHO + OH\ (+ O_2/NO, +M) \rightarrow OCH_2CH(OH)CHO + NO_2$$

By analogy with the β-hydroxy alkoxy radicals resulting from the reaction of OH with methacrolein ($CH_2{=}C(CH_3)CHO$),[27,28] and with the general behavior of β-hydroxy alkoxy radicals, the above radicals are likely to decompose:

$$HOCH_2CH(O)CHO\ (+M) \rightarrow HOCH_2CHO + HCO$$

$$\rightarrow CHOCHO + CH_2OH$$

$$CH_2OH + O_2 \rightarrow HCHO + HO_2$$

$$HCO + O_2 \rightarrow HO_2 + CO$$

$$OCH_2CH(OH)CHO\ (+M) \rightarrow HCHO + HOCHCHO$$

$$HOCHCHO + O_2 \rightarrow CHOCHO + HO_2$$

The decomposition of the β-hydroxy alkoxy radical resulting from the OH addition to the terminal carbon leads to glycolaldehyde and glyoxal as stable products while that of the other β-hydroxy alkoxy radical leads to formaldehyde and HOCHCHO. This latter radical leads to glyoxal through its reaction with O_2. It can be noticed that CO might be formed as primary product through the reaction of HCO with O_2.

From the observed products, it was not possible to determine the branching ratio of the H-atom abstraction and of the OH addition to the double bond since both pathways can lead to the same products, glyoxal and formaldehyde. However, the detection of peroxynitrate and that of glycolaldehyde suggest that both reaction pathways occur. The averaged obtained yield for glycolaldehyde of (20 ± 10)% indicates that the branching ratio of the addition channel is at least of the same order. Assuming that all glyoxal is produced through the addition channel, one can estimate that about 25% of the reaction of OH with acrolein goes through the addition of OH to the double bond. Most of this addition would occur on the terminal carbon ($CH_2{=}$). Unfortunately, we were not able to quantify the observed peroxynitrate which would enable us to estimate the branching ratio of the abstraction channel with more accuracy. In their study of the OH-initiated oxidation of acrolein, Grosjean et al.[18] have reported the same products as those observed in this work but were not able to estimate the relative importance of OH addition and abstraction pathways.

(ii) trans-Crotonaldehyde. **(a) Laboratory Studies.** Mixtures of 50−150 ppm of *trans*-crotonaldehyde and 8−63 ppm of NO were irradiated in the presence of H_2O_2 for 50−150 min. The observed primary products were glyoxal and acetaldehyde, and formaldehyde, formic acid, and CO were detected as secondary products. In addition, FTIR analysis indicated the presence of $CH_3C(O)O_2NO_2$ (PAN) as secondary product and another PAN-type compound assumed to be $CH_3CH{=}CHC(O)O_2NO_2$. Acetaldehyde was the main oxidation product, but its formation yield could not be derived since it was reaction-time dependent. Glyoxal, the other primary product, was formed with an initial yield of (16 ± 4)%.

(b) EUPHORE Studies. Two experiments have been performed with initial *trans*-crotonaldehyde mixing ratios of 1.5 and 1.8 ppm in the presence of 150 and 110 ppb of NO_x, respectively. After exposure of the reaction mixtures to sunlight for 6 h, the observed reaction products were identical to those detected in the laboratory. The primary reaction products were glyoxal with a yield of (16 ± 2)% and acetaldehyde with an initial yield of (30 ± 5)%. In both experiments, high amounts of CO were measured (up to 1.3 and 1.5 ppm). The other observed products were formaldehyde, formic acid, PAN, and another PAN-type compound. Sampling using DNPH cartridges confirmed the presence of glyoxal and acetaldehyde and indicated the presence of another carbonyl compound which might be methylglyoxal ($CH_3C(O)CHO$) or methylglycolaldehyde ($CH_3CH(OH)CHO$). The concentration-time profiles of HCHO and HCOOH indicated that these two compounds were not primary reaction products, as it can be seen from Figure 5. However, it has to be mentioned that the carbon balance at the end of the experiment was only about 55%, indicating the possible presence of other compounds that could not be identified and quantified.

Similarly to methacrolein, the reaction of OH with *trans*-crotonaldehyde is expected to proceed mainly by both OH-addition to the carbon−carbon double bond and H-abstraction of the aldehydic hydrogen, the abstraction from the methyl group being negligible.[27,28] The overall mechanism is comparable to that of the OH-initiated oxidation of acrolein presented above. The H-abstraction channel may lead to the formation of the $CH_3CH{=}CHC(O)O_2$:

$$CH_3CH{=}CHCHO + OH \rightarrow CH_3CH{=}CHCO + H_2O$$

$$CH_3CH{=}CHCO\ (+ O_2, + M) \rightarrow CH_3CH{=}CHC(O)O_2$$

As it was the case for acrolein, depending on the ratio $[NO_2]/[NO]$, $CH_3CH{=}CHC(O)O_2$ will form $CH_3CH{=}CHC(O)O_2NO_2$ or $CH_3CH{=}CHC(O)O$:

$$CH_3CH{=}CHC(O)O_2 + NO_2\ (+M) \rightarrow CH_3CH{=}CHC(O)O_2NO_2$$

$$CH_3CH{=}CHC(O)O_2 + NO \rightarrow CH_3CH{=}CHC(O)O + NO_2$$

The $CH_3CH{=}CHC(O)O$ radical decomposes and leads to $CH_3CH{=}CH$ and CO_2:

$$CH_3CH{=}CHC(O)O\ (+M) \rightarrow CH_3CH{=}CH + CO_2$$

Alternatively, $CH_3CH{=}CHCO$ may decompose, forming $CH_3CH{=}CH$ and CO:

$$CH_3CH{=}CHCO\ (+M) \rightarrow CH_3CH{=}CH + CO$$

Analogous to the acrolein degradation, the following processes could occur:

$$CH_3CH{=}CH + O_2/NO\ (+M) \rightarrow CH_3CH{=}CHO + NO_2$$

$$CH_3CH{=}CHO + O_2 \rightarrow [CH_3C(OO)H{=}CHO]$$

$$[CH_3C(OO)H{=}CHO] \rightarrow CH_3COCHO + OH$$

$$\rightarrow CH_3CHO + CO + OH$$

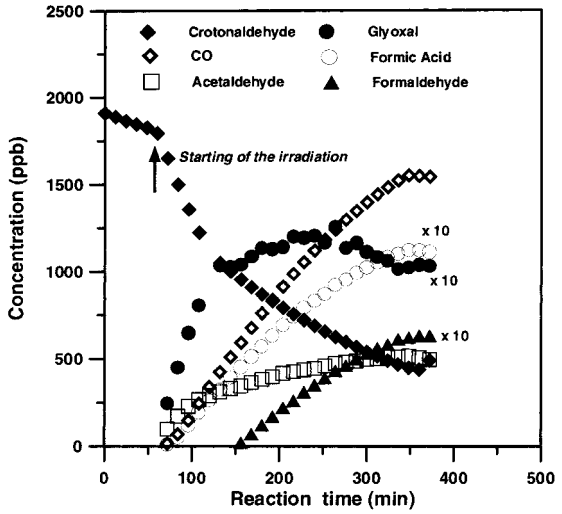

Figure 5. OH-initiated oxidation of *trans*-crotonaldehyde, experimental concentration profiles of the reactant and products (at EUPHORE).

alternatively,

$$CH_3CH{=}CHO \leftrightarrow CH_3C(HO){=}CH$$

$$CH_3C(HO){=}CH + O_2\ (+M) \rightarrow CH_3C(HO){=}CHO_2$$

$$CH_3C(HO){=}CHO_2 \rightarrow HCO + CH_3COOH$$

$$\rightarrow CH_3COCHO + OH$$

$$HCO + O_2 \rightarrow HO_2 + CO$$

Both $CH_3CH{=}CHC(O)O_2NO_2$ and CO were observed as products of the reaction, indicating that the $CH_3CH{=}CHC(O)O_2$ radical might react with both NO and NO_2 in our system. However, the observed CO could be also a product of the addition channel, formed through reaction of HCO with O_2 as shown below. Orlando et al.[28] suggested that the decomposition of the peroxy radical $CH_2{=}C(CH_3)O_2$ formed in the degradation of methacrolein leads to CH_3, HCHO, and CO. Similar decomposition of the peroxy radical ($CH_3CH{=}CHO_2$) produced in the degradation of *trans*-crotonaldehyde cannot be ruled out.

The addition channel of OH to the carbon−carbon double bond leads to two β-hydroxy alkoxy radicals which decompose similarly to acrolein and methacrolein:

$$CH_3CH{=}CHCHO + OH\ (+ O_2/NO, +M) \rightarrow CH_3CH(OH)CH(O)CHO + NO_2$$

$$CH_3CH_2{=}CHCHO + OH\ (+ O_2/NO, +M) \rightarrow CH_3CH(O)CH(OH)CHO + NO_2$$

$$CH_3CH(OH)CH(O)CHO\ (+M) \rightarrow CH_3CH(OH)CHO + HCO$$

$$\rightarrow CH_3CH(OH) + CHOCHO$$

$$CH_3CH(O)CH(OH)CHO\ (+M) \rightarrow CH_3CHO + CH(OH)CHO$$

The stable products from this scheme are methylglycolaldehyde ($CH_3CH(OH)CHO$) and glyoxal from the first β-hydroxy alkoxy radical and acetaldehyde from the second one. HCO, $CH_3CH(OH)$, and CH(OH)CHO radicals lead, through their reactions with O_2, to the formation of CO, CH_3CHO, and CHOCHO, respectively. All these compounds were detected except methylglycolaldehyde. However, HPLC analysis showed the presence of an unidentified carbonyl compound which could be methylglycolaldehyde or methylglyoxal, this latter being produced in the H-abstraction channel.

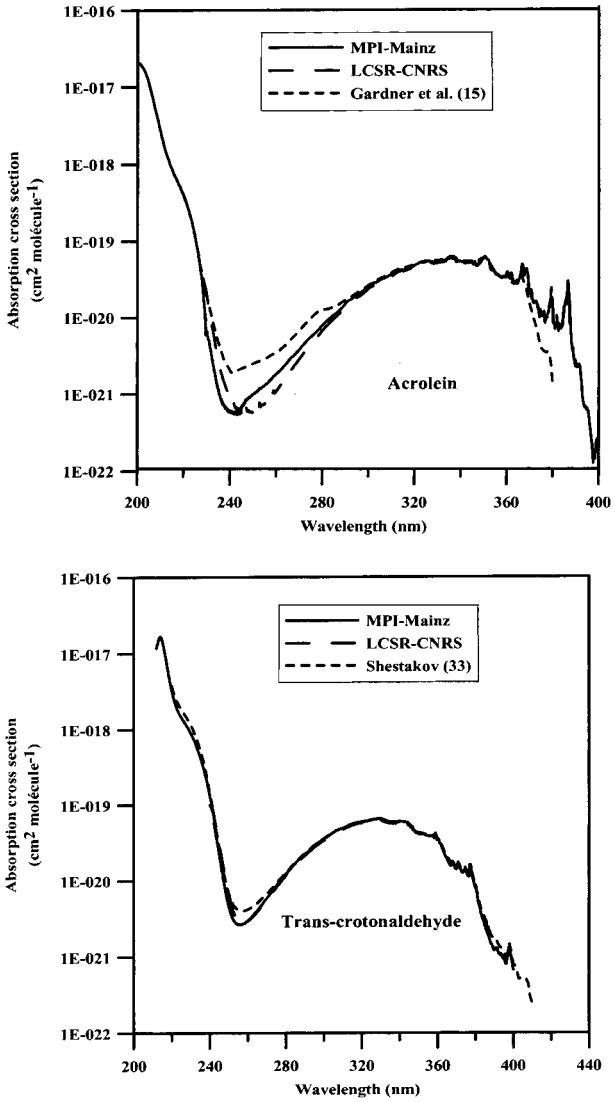

Figure 6. UV−visible absorption spectra of acrolein and *trans*-crotonaldehyde.

Both abstraction and addition channels lead to the same products as shown above, except the PAN-type compound which is exclusively formed through the abstraction channel. This made it difficult for us to derive the branching ratio of the reaction of OH with *trans*-crotonaldehyde.

UV-Absorption Spectra. The obtained absorption spectra of acrolein and *trans*-crotonaldehyde are shown in Figure 6, along with those reported in the literature. Both spectra display a broad absorption band between 250 and 400 nm, which is slightly structured at wavelengths above 360 nm. Below 250 nm, features of a much stronger absorption band are observed. The spectra of acrolein and *trans*-crotonaldehyde are very similar in terms of peak positions, cross sections, and bandwidths. For both species, the maximal cross sections (except the strong absorption before 250 nm) are reached around 330 nm ($\sigma \approx 6.4 \cdot 10^{-20}$ cm^2 molecule^{-1}) for *trans*-crotonaldehyde and around 336 nm ($\sigma \approx 6.3 \cdot 10^{-20}$ cm^2 molecule^{-1}) for acrolein. This absorption can be assigned to the $n \rightarrow \pi^*$ transition.

TABLE 4: Absorption Cross-sections of Acrolein and *trans*-Crotonaldehyde at 298 ± 2 K (10^{-20} cm^2 molecule^{-1})[a]

λ (nm)	acrolein σ	*trans*-crotonaldehyde σ	λ (nm)	acrolein σ	*trans*-crotonaldehyde σ
256		0.27	324	5.17	6.06
258		0.28	326	5.34	6.22
260		0.30	328	5.20	6.39
262		0.33	330	5.31	6.45
264		0.37	332	5.44	6.10
266		0.42	334	5.80	5.87
268		0.49	336	6.24	5.84
270		0.57	338	5.46	5.77
272		0.66	340	5.31	5.88
274		0.77	342	5.10	5.77
276		0.90	344	5.12	5.73
278		1.03	346	5.30	5.05
280		1.18	348	5.17	4.51
282	0.84	1.35	350	5.94	4.13
284	0.97	1.54	352	5.79	4.06
286	1.08	1.74	354	4.18	3.88
288	1.23	1.95	356	3.63	3.88
290	1.46	2.16	358	3.28	3.79
292	1.62	2.40	360	3.92	3.45
294	1.80	2.66	362	3.72	2.96
296	1.97	2.93	364	2.86	2.12
298	2.18	3.18	366	3.74	1.76
300	2.47	3.44	368	3.82	1.69
302	2.70	3.71	370	2.17	1.43
304	2.85	4.02	372	1.58	1.46
306	3.09	4.33	374	1.14	1.37
308	3.29	4.58	376	1.14	1.16
310	3.59	4.79	378	1.24	1.25
312	3.92	5.05	380	1.10	0.81
314	4.15	5.32	382	0.84	0.48
316	4.21	5.58	384	0.79	0.32
318	4.47	5.77	386	1.81	0.24
320	4.65	5.85	388	0.49	0.17
322	5.08	5.93	390	0.25	0.14

[a] Average between MPI values and LCSR values.

The UV−visible absorption cross sections of acrolein and *trans*-crotonaldehyde obtained in both laboratories (Orléans and Mainz) are averaged and given in Table 4, in 2 nm intervals. Agreement is obtained between the spectra measured at MPI and at LCSR/CNRS over the wavelength range 255−390 nm for *trans*-crotonaldehyde and 280−390 nm for acrolein. However, a significant deviation around 250 nm is observed for acrolein, where the spectrum of LCSR is shifted to the higher wavelengths. The spectra of Gardner et al.,[15] which was scanned from their article and integrated every nanometer, is similar to that obtained in this work between 280 and 370 nm but deviates at the other wavelengths.

The spectra of *trans*-crotonaldehyde obtained at LCSR/CNRS, at MPI and by Shestakov,[33] display the same shape, except for wavelengths around 270 nm where the cross sections obtained at MPI and LCSR/CNRS are slightly different and those reported by Shestakov which are 25-35% lower than ours.

Photolysis Investigation. *Laboratory Studies.* **(i) Acrolein**. The experimental conditions and the obtained photolysis removal rates are summarized in Table 5. Mixtures of 9−49 mTorr of acrolein in synthetic air were irradiated during typically 90 min with TL12 lamps at different pressures (100, 300, 500, and 700 Torr) and at (298 ± 2) K. The FTIR analysis was conducted using the acrolein band in the range 1688−1755 cm^{-1}. While no change in the concentration of acrolein was observed in the dark, indicating that thermal dissociation or wall loss of acrolein was negligible in our experimental conditions, a small decrease (2−10) % was observed with the lamps on. The removal rate was found to be pressure independent in the range 100−700 Torr. The total removal rate, derived from the nine experiments performed at different pressures, is $k_{\text{removal}} = (1.5 \pm 0.3) \cdot 10^{-5}$ s^{-1}.

The possible photolysis channels are the following:[15]

$$CH_2{=}CHCHO + h\nu \rightarrow CH_2{=}CH + HCO$$

$$\rightarrow CH_2{=}CH_2 + CO$$

$$\rightarrow CH_2{=}CHCO + H$$

CH_2=CH, HCO, and H will react with O_2 whereas CH_2=CHCO may react with O_2 or decompose. The stable end products would be CO, CH_2=CH_2, HCHO, CHOCHO, and probably others. However, no photolysis products could be observed in the FTIR spectra, indicating that any product formed was below the detection limit in our experimental conditions; therefore, no conclusion could be drawn about the possible photolysis channels. This suggests that the overall quantum yield for dissociation within the overlapping absorption band is very low. A quantum yield of 0.033 was calculated from the known photolysis rates of acrolein and Cl_2, which was used as an actinometer, taking into account the overlap integrals of the TL12 lamp spectrum and the absorption spectra of both compounds.

Photolysis of acrolein has been the subject of several previous studies (see Gardner et al.[15] and references therein). The most recent work is that of Gardner et al.,[15] who studied the photodecomposition at 313 and 334 nm in the pressure range 26−760 Torr of O_2–N_2 mixtures. These authors found that the photolysis was very inefficient at both wavelengths at high pressure but increases at low pressure. At 313 nm, the quantum yields of acrolein loss was found to be described reasonably well by the following: $1/(\phi_d - 0.004) = 0.086 + 1.613 \cdot 10^{-17}$ [M] for $8 \cdot 10^{17} < [M] < 2.6 \cdot 10^{19}$ (molecule cm^{-3}), where ϕ_d is the photodissociation quantum yield (the experimental results were $\phi_d = 6.5 \cdot 10^{-3}$ at 1 atm and $\phi_d = 8.1 \cdot 10^{-2}$ at 26 Torr).

TABLE 5: Experimental Conditions and Photolysis Removal Rates for Acrolein and *trans*-Crotonaldehyde in Air Obtained in the Laboratory

[acrolein] (mTorr)	pressure (Torr)	removal rate (s^{-1})	[*trans*-crotonaldehyde] (mTorr)	pressure (Torr)	removal rate (s^{-1})
43.7	100	$(1.46 \pm 0.08) \cdot 10^{-5}$	9.4	100	$(1.19 \pm 0.12) \cdot 10^{-4}$
44.6	100	$(1.87 \pm 0.11) \cdot 10^{-5}$	9.5	100	$(1.34 \pm 0.16) \cdot 10^{-4}$
9.2	300	$(1.69 \pm 0.32) \cdot 10^{-5}$	50.6	100	$(1.40 \pm 0.15) \cdot 10^{-4}$
45.6	300	$(1.45 \pm 0.06) \cdot 10^{-5}$	46.9	100	$(1.45 \pm 0.13) \cdot 10^{-4}$
45.4	300	$(1.20 \pm 0.09) \cdot 10^{-5}$	47.1	100	$(1.18 \pm 0.14) \cdot 10^{-4}$
44.3	500	$(1.47 \pm 0.07) \cdot 10^{-5}$	9.5	300	$(1.48 \pm 0.14) \cdot 10^{-4}$
43.8	700	$(1.04 \pm 0.12) \cdot 10^{-5}$	8.7	700	$(1.25 \pm 0.18) \cdot 10^{-4}$
43.4	700	$(1.88 \pm 0.25) \cdot 10^{-5}$	9.1	700	$(1.27 \pm 0.12) \cdot 10^{-4}$
43.5	700	$(1.14 \pm 0.07) \cdot 10^{-5}$	9.4	700	$(1.26 \pm 0.14) \cdot 10^{-4}$
			46.0	700	$(1.06 \pm 0.14) \cdot 10^{-4}$
			45.6	700	$(1.07 \pm 0.15) \cdot 10^{-4}$

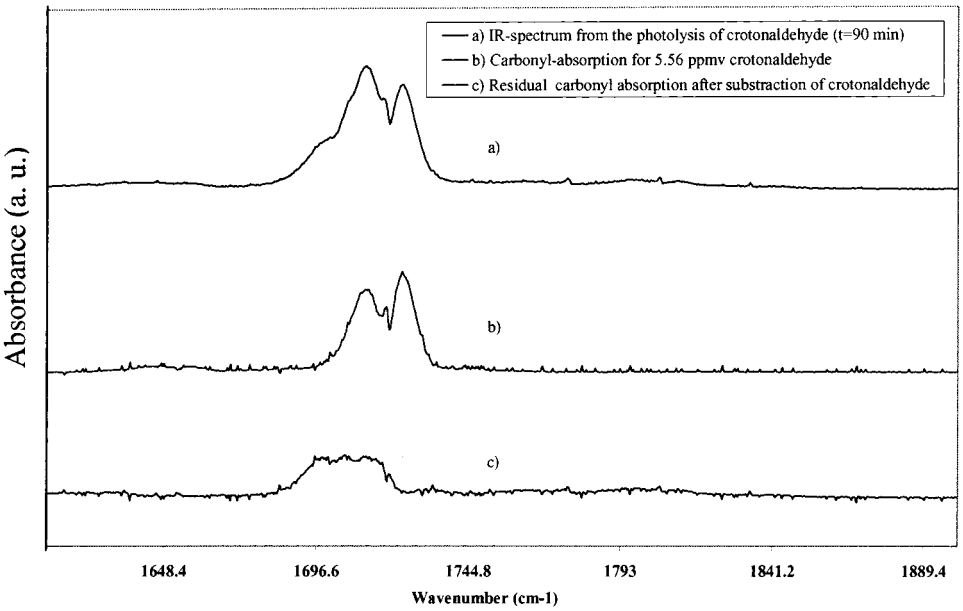

Figure 7. Residual spectrum from photolysis of *trans*-crotonaldehyde.

The quantum yields of most observed products were also dependent on the total pressure, indicating the complexity of the mechanisms leading to these products, according to the authors. The dominant products detected by GC were CO and C_2H_4; their quantum yields were found to be quenched to small fractions at high pressure. Other compounds such as HCHO, CHOCHO, CO_2, and CH_3OH were also identified. The photolysis experiments performed at 334 nm by these authors indicated that the photodecomposition of acrolein as well as the observed product quantum yields were less than that at 313 nm.

The other previous studies of the photolysis of acrolein were performed at different wavelengths, 313 nm,[17,34,35] 253.7 nm,[36] and at short wavelengths (i.e., 193 nm).[37−39] Most of these studies reported that the photolysis of acrolein was a slow process, and CO and C_2H_4 were detected among the observed products. A complete discussion of the these later studies can be found elsewhere.[15]

(ii) *trans*-Crotonaldehyde. Similarly to acrolein, mixtures of 8−51 mTorr of *trans*-crotonaldehyde in 100−700 Torr of synthetic air were irradiated for typical periods of 90 min at room temperature. The IR band used for integration was 1036−1188 cm^{-1}. The experimental conditions and the obtained removal rates of *trans*-crotonaldehyde are presented in Table 5. No change in the concentration of *trans*-crotonaldehyde was observed in the dark, indicating that thermal dissociation or wall loss of *trans*-crotonaldehyde was negligible. Typically about 45% of *trans*-crotonaldehyde was consumed during the photolysis.

Concerning the photolytic products, the spectral subtraction of the remaining *trans*-crotonaldehyde lead to a residual spectral feature showing some carbonyl absorption bands (1690−1740 cm^{-1}) slightly shifted to smaller wavenumbers (1680−1725 cm^{-1}) as shown in Figure 7. From the 11 experiments performed under different conditions, the following average value of the "removal rate" of *trans*-crotonaldehyde was derived: $k_{removal} = (1.3 \pm 0.2) \cdot 10^{-4}$ s^{-1}, nearly an order of magnitude larger than was observed for acrolein. A quantum yield of 0.23 was calculated for the disappearance of *trans*-crotonaldehyde using Cl_2 as an actinometer:

The possible photolysis channels are

$$CH_3CH{=}CHCHO + h\nu \rightarrow CH_3CH{=}CH + HCO$$

$$\rightarrow CH_3CH{=}CH_2 + CO$$

$$\rightarrow CH_3 + CH{=}CHCHO$$

$$\rightarrow CH_3CH{=}CHCO + H$$

The formed radicals such as HCO, CH_3, and H would be rapidly scavenged by reaction with O_2 whereas $CH_3CH{=}CH$, $CH{=}CHCHO$ and $CH_3CH{=}CHCO$ may react with O_2 or decompose. Ultimately, stable compounds such as CO, CH_3OH, HCHO, $CH_3CH(O)CHO$, $CH_3CH{=}CH_2$, and probably others will be formed. However, none of the above products was observed, indicating that the photolysis channels given above do not occur in our experimental conditions or the corresponding products are below the detection limit of our system. However, the residual spectra indicate the presence of a product having a spectrum different from those of the above stable products. This leads us to speculate that the carbonyl absorption bands in the residual spectra might be due to an unidentified polymeric compound as suggested by Allen and Pitts[16] and Coomber and Pitts.[17] It may also be attributed to a photoisomerization process: *trans*-crotonaldehyde ↔ *cis*-crotonaldehyde, *trans*-crotonaldehyde ↔ enol-crotonaldehyde. In the absence of IR spectra of these products, we are not able to distinguish between these possibilities.

The previous studies have shown that the photolysis of *trans*-crotonaldehyde is a slow process at room temperature in the wavelength range of atmospheric interest; see elsewhere.[16,17] However, photoisomerization of *trans*-crotonaldehyde has been reported by Coomber et al., who detected enol-crotonaldehyde during their experiments at 303 K in the wavelength range 253−313 nm.[40] This process was observed to be independent of the concentration of the *trans*-crotonaldehyde and light intensity. The isomerization to but-3-en-al was also reported by McDowell and Sifniades in the wavelentgh range 245−400 nm at room

TABLE 6: Experimental Conditions and Obtained Data for the Photolysis of Acrolein and *trans*-Crotonaldehyde at EUPHORE[a]

aldehyde	concentration (ppm)	tracer or scanvenger (ppm)	k_{total} (s^{-1})	k_{SF6} (s^{-1})	k_{tracer} (s^{-1})	J (s^{-1})
acrolein	0.95	DNBE (0.129)	$6.5 \cdot 10^{-6}$	$7.4 \cdot 10^{-6}$	$7.1 \cdot 10^{-6}$	$<2 \cdot 10^{-6}$
	0.88	C-hexane (26.8)	$1.01 \cdot 10^{-5}$	$9.9 \cdot 10^{-6}$		$<2 \cdot 10^{-6}$
trans-crotonaldehyde	1.34	C-hexane (51.3)	$1.73 \cdot 10^{-5}$	$7.1 \cdot 10^{-6}$		$1.0 \cdot 10^{-5}$
	1.45	DNBE (0.129)	$2.20 \cdot 10^{-5}$	$6.9 \cdot 10^{-6}$	$8.2 \cdot 10^{-6}$	$1.4 \cdot 10^{-5}$

[a] C-hexane = cyclohexane; DNBE = di-*n*-butyl ether; k_{total} is the total removal rate of the aldehyde; k_{SF6} is the dilution rate; k_{tracer} is the tracer removal rate; J is the photolysis rate.

temperature.[41] It has been also suggested that the only room-temperature process was a photopolymerization; see Allen and Pitts.[16]

EUPHORE Studies. Two experiments were conducted for each aldehyde, one in the presence of the tracer and the other in the presence of the scavenger. The analysis of the reactants and products were performed using FTIR, GC (FID/PID/TGA), and HPLC.

(i) Acrolein. The experimental conditions and the photolysis rates obtained in the two experiments are given in Table 6. The initial concentrations of acrolein were 0.88 and 0.95 ppm. The obtained total loss rate of acrolein, k_{tot}, was close to that of the dilution rate (first-order decay rate of SF_6), indicating that, under our experimental conditions, the only measurable loss process is dilution. From these measurements, only an upper limit could be derived: $J_{acro} < 2 \cdot 10^{-6}$ s^{-1}. While no product could be observed by FTIR, the HPLC analysis of samples collected on DNPH-cartridges showed, at the end of the experiment, the presence of very small amounts of HCHO (7 and 8 ppb), acetaldehyde (6 and 8 ppb), and glyoxal (4 and 8 ppb). However, CO could also be produced from the photolysis of compounds such as formaldehyde and glyoxal. Hence, the level of these latter aldehydes could be considered as a lower limit. We cannot conclude on the presence of C_2H_4 since we were not able to distinguish its IR absorption bands from those of SF_6 and acrolein. The above products were also reported by Gardner et al.,[15] indicating that the proposed photolysis channels may all occur in the atmospheric conditions.

The obtained photolysis rate (J_{acro}) can be used to calculate the effective quantum yield of acrolein according to the following formula:

$$J = \int \sigma(\lambda) \cdot \phi(\lambda) \cdot I(\lambda) \cdot d\lambda \ (290-400 \text{ nm})$$

where $\sigma(\lambda)$ is the absorption cross section (cm^2 $molecule^{-1}$), $\phi(\lambda)$, the quantum yield, and $I(\lambda)$, the actinic flux (photons cm^{-2} s^{-1}). Using the Luther model,[42] for a latitude of 30° north, at ground level, no clouds in July, we have calculated $J_{calc} = 4.3 \cdot 10^{-4}$ s^{-1} assuming quantum yield of unity. The effective quantum yield for acrolein photolysis, defined as J_{exp}/J_{cal}, of $\phi_{eff} \leq 0.005$ is derived with $J_{exp} < 2 \cdot 10^{-6}$ s^{-1} (for midday conditions). The measured $J(NO_2)$ during the two experiments was around $9 \cdot 10^{-3}$ s^{-1}.

(ii) *trans*-Crotonaldehyde. The experimental conditions as well as the obtained decay rates are reported in Table 6. Only the data using GC analysis are shown in this table, the FTIR data were highly variable depending on the IR band used for analysis (966−977 and 2620−2768 cm^{-1}), and the reason for that is not clear to us.

The derived average value of the "photolysis" rate from the two experiments is $(1.2 \pm 0.2) \cdot 10^{-5}$ s^{-1} (Figure 8). Similarly to what was observed in the laboratory, there was a distinguishable removal of *trans*-crotonaldehyde but no characteristic product formation in noticeable amount besides acrolein which

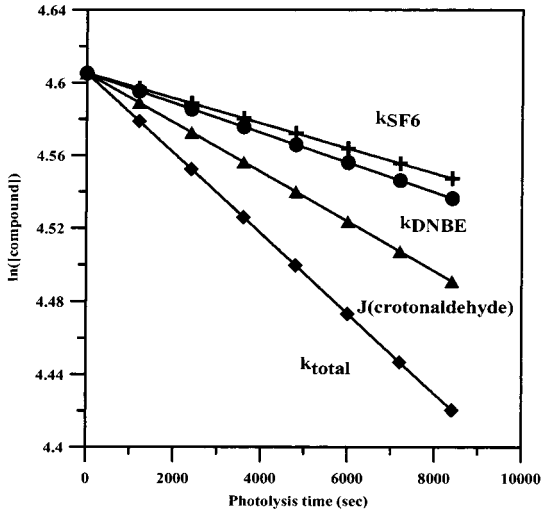

Figure 8. Photolysis of *trans*-crotonaldehyde at EUPHORE.

was detected by HPLC in the two experiments (15 and 22 ppb, respectively), HCHO, CH_3CHO, CHOCHO, and H_2O_2 which were detected by GC or HPLC in the ppb range. Acrolein could be formed during the photolysis of the isomer of *trans*-crotonaldehyde $CH_2{=}CHCH_2CHO$. An IR band at 1108 cm^{-1} was observed but could not be attributed. Possibly, a fast isomerization of *trans*-crotonaldehyde occurs during the irradiation, and the observed removal of *trans*-crotonaldehyde is that due to this isomerization as suggested by the laboratory studies. If this is the case, the measured "photolysis" rate is that due to both photoisomerization and photolysis. The measured value of $(1.2 \pm 0.2) \cdot 10^{-5}$ s^{-1} represents then an upper limit for the photolysis rate in our experimental conditions.

Assuming a photolysis quantum yield of unity, $\phi = 1$, we have calculated the photolysis rate; using the same expression as that used for acrolein and under the same conditions, we obtained: $J_{calc} = 4.0 \cdot 10^{-4}$ s^{-1}. This enabled us to calculate an effective quantum yield for *trans*-crotonaldehyde photolysis using the photolysis rate obtained experimentally ($J_{exp} < (1.2 \pm 0.2) \cdot 10^{-5}$ s^{-1}), of $\phi_{eff} < 0.030 \pm 0.006$.

This work reports for the first time the photolysis rates and products of acrolein and *trans*-crotonaldehyde under natural sunlight irradiation. The obtained results from the experiments performed at EUPHORE indicates that the photolytic decomposition of these two unsaturated aldehydes is slow which is in agreement with the data obtained under the laboratory conditions from this work and the previous studies at room temperature. Our results combined with others for the photolysis of acrolein, *trans*-crotonaldehyde, and methacrolein ($CH_2{=}C(CH_3)CHO$) show that α, β unsaturated aldehydes are photolytically stable under atmospheric conditions.[20,43] Gierczak et al. reported an upper limit for the methacrolein photolysis quantum yield of 0.01 at 308, 337, and 351 nm.[43] This photostability of α, β unsaturated aldehydes is probably due to a resonance stabilization.

Atmospheric Implications. In addition to reaction with OH and photolysis, acrolein and *trans*-crotonaldehyde can be removed from the atmosphere by reaction with NO_3 and O_3 or by wet deposition. Considering the gas-phase loss processes, the lifetimes toward reaction with OH, NO_3, and O_3 and toward photolysis have been calculated for the two aldehydes. These lifetimes, calculated using the expressions $\tau_X = 1/k_X[X]$ with X = OH, NO_3, O_3, and $\tau_J = 1/J$, are as follows:

	OH	NO_3	O_3	J
acrolein	7 hours	14 months	36 days	>6 days
trans-croton-aldehyde	4 hours	83 days	5 days	>1 day

In the above calculations, the following rate constant values have been used: $k_{OH} = 2 \cdot 10^{-11}$ (this work), $k_{NO3} = 1.1 \cdot 10^{-15}$,[6] $k_{O3} = 2.6 \cdot 10^{-19}$ cm^3 molecule^{-1} s^{-1},[44] and $J < 2 \cdot 10^{-6}$ s^{-1} (this work) for acrolein; $k_{OH} = 3.4 \cdot 10^{-11}$ (this work), $k_{NO3} = 5.6 \cdot 10^{-15}$,[6] $k_{O3} = 1.74 \cdot 10^{-18}$,[10] cm^3 molecule^{-1} s^{-1}, and $J < 1.2 \cdot 10^{-5}$ s^{-1} (this work) for *trans*-crotonaldehyde. The atmospheric concentrations used, $[OH] = 2 \cdot 10^6$ molecule cm^{-3}, $[NO_3] = 2.5 \cdot 10^7$ molecule cm^{-3} (10 pptv), and $[O_3] = 1.25 \cdot 10^{12}$ molecule cm^{-3} (50 ppbv), are typical of continental lower troposphere. The OH concentration corresponds to a 12 h averaged value which is applicable to lifetimes less than 1 day.[45] The other possible atmospheric loss process for the two aldehydes is wet deposition. The low values of Henry's law solubility constant reported by Meylan and Howard[46] for acrolein and *trans*-crotonaldehyde, 8.2 and 51 M atm^{-1}, respectively, may imply that wet deposition is not an important removal process for these two compounds.

The calculated lifetimes show that the OH reaction is the major loss process for both aldehydes. These short lifetimes indicate that these aldehydes will be degraded close to their sources. The products formed from the OH-initiated oxidation are mainly lighter carbonyl compounds, which are net sources of HO_x (OH, HO_2) radicals that enhance photooxidant formation. Besides, the unsaturated PAN-type compounds, vinyl PAN and methyl-vinyl PAN, also formed from acrolein and *trans*-crotonaldehyde, respectively, may not be efficient NO_x reservoirs of saturated PANs, as a result of the expected significant reactivity through OH addition to the C=C double bond.

Acknowledgment. The EU through RADICAL project (ENV4-CT97-0419), the French Ministry of Environment through the PRIMEQUAL-PREDIT program, and CNRS through the PNCA program are acknowledged for support. The authors thank Karl-Heinz Möbus (MPI-Mainz) for the calculation of quantum yields and N. Jensen and R. Winterhalter for their assistance at Euphore. Fundación CEAM is supported by the Generalitat Valenciana and Fundación BANCAIXA.

References and Notes

(1) Graedel, T. E.; Hawkins, D. T.; Claxton, L. D. *Atmospheric Chemical Compounds: Sources, Occurrence and Bioassay*, Academic Press: Orlando, 1986.
(2) http://www.epa.gov.
(3) Grosjean, D. *J. Air Waste Manag. Assoc.* **1990**, *40*, 1664−1668.
(4) Agency for Toxic Substances and Disease Registry (ATSDR), Toxicological Profile for Acrolein. U. S. Public Health Service, U.S. Department Health and Human Services, Atlanta, GA., 1989.
(5) Atkinson, R.; Aschmann, S. M.; Goodman, M. A. *Int. J. Chem. Kinet.* **1987**, *19*, 299−307.
(6) Atkinson, R. *J. Phys. Chem. Ref. Data* **1991**, *20*, 459−507.
(7) Atkinson, R.; Aschmann, S. M.; Winer, A. M.; Pitts, J. N., Jr. *Int. J. Chem. Kinet.* **1981**, *13*, 1133−1142.
(8) Treacy, J.; El Hag, M.; O'Farrell, D.; Sidebottom, H. *Ber. Bunsen-Ges. Phys. Chem.* **1992**, *96*, 422−427.
(9) Grosjean, D.; Grosjean, E.; Williams, E. L., II. *Int. J. Chem. Kinet.* **1993**, *25*, 783−794.
(10) Grosjean, E.; Grosjean, D. *Int. J. Chem. Kinet.* **1998**, *30*, 21−29.
(11) Maldotti, A.; Chiorboli, C.; Bignozzi, C. A.; Bartocci, C.; Carassiti, V. *Int. J. Chem. Kinet.* **1980**, *12*, 905−913.
(12) Kerr, J. A.; Sheppard, D. W. *Environ. Sci. Technol.* **1981**, *15*, 960−963.
(13) Atkinson, R.; Aschmann, S. M.; Pitts, J. N. *Int. J. Chem. Kinet.* **1983**, *15*, 75−81.
(14) Edney, E. O.; Kleindienst, T. E.; Corse, E. W. *Int. J. Chem. Kinet.* **1986**, *18*, 1355−1371.
(15) Gardner, E. P.; Sperry, P. D.; Calvert, J. G. *J. Phys. Chem.* **1987**, *91*, 1922−1930.
(16) Allen, E. R.; Pitts, J. N. *J. Am. Chem. Soc.* **1969**, *91* (12), 3135−3139.
(17) Coomber, J. W.; Pitts, J. N. *J. Am. Chem. Soc.* **1969**, *91* (18), 4955−4960.
(18) Grosjean, E.; Williams, E. L.; Grosjean, D. *Sci. Total Environ.* **1994**, *153*, 195−202.
(19) Mellouki, A.; Téton, S.; Laverdet, G.; Quilgars, A.; Le Bras, G. *J. Chim. Phys.* **1994**, *91*, 473−487.
(20) Raber, W. H.; Moortgat, G. K. *Progress and Problems in Atmospheric Chemistry*; Singapore, Ed. J. Baker, World scientific Publ. Co., 1996: 318−373.
(21) Becker, K. H., Ed. *The European Photoreactor EUPHORE*, Final Report of the EC Project EV5V-CT92-0059; Wuppertal, 1996.
(22) Barnes, I.; Wenger J., Eds. *EUPHORE Report 1997*, Institute of Physical Chemistry; Bergische Universitat Wuppertal, Wuppertal, 1998.
(23) Semadeni, M.; Stocker, D. W.; Kerr, J. A. *J. Atm. Chem.* **1993**, *16*, 79−93.
(24) Semmes, D. H.; Ravishankara, A. R.; Gump-Perkins, C. A.; Wine, P. H. *Int. J. Chem. Kinet.* **1985**, *17*, 303−313.
(25) Thévenet, R.; Mellouki, A.; Le Bras, G. *Int. J. Chem. Kinet.* **2000**, *32*, 676−685.
(26) Dobé, S.; Khachatryan, L. A.; Berces, T. *Ber. Bunsen-Ges. Phys. Chem.* **1989**, *93*, 847−852.
(27) Tuazon, E. C.; Atkinson, R. *Int. J. Chem. Kinet.* **1990**, *22*, 591−602.
(28) Orlando, J. J.; Tyndall, G. S.; Paulson, S. E. *Geophys. Res. Lett.* **1999**, *26*, 2191−2194.
(29) Kwok, E. S. C.; Atkinson, R. *Atmos. Environ.* **1995**, *29*, 1685−1695.
(30) Gutman, D.; Nelson, H. H. *J. Phys. Chem.* **1985**, *87*, 3902−3905.
(31) Zhu, L.; Johnston, G. *J. Phys. Chem.* **1995**, *99*, 15114−15119.
(32) Lesclaux, R., private communication.
(33) Shestakov, O. The Annual Meeting of the Bunsengesellshaft fur Physikalische Chemie, Dortmund, 13−15 May, 1999.
(34) Thompson, H. W.; Linett, J. W. *J. Am. Chem. Soc.* **1935**, *57*, 2.
(35) Blacet, F. E.; Fielding, G. H.; Roof, J. G. *J. Am. Chem. Soc.* **1937**, *59*, 2375.
(36) Harrison, H. G.; Lossing, F. B. *Can. J. Chem.* **1959**, *37*, 1696.
(37) Umstead, M. E.; Shortridge, R. G.; Lin, M. C. *J. Phys. Chem. Phys.* **1978**, *82*, 1455−1460.
(38) Fujimoto, G. T.; Umstead, M. E.; Lin, M. C. *J. Chem. Phys.* **1985**, *82*, 3042−3044.
(39) Shinohara, H.; Nishi, N. *J. Chem. Phys.* **1982**, *77*, 234−245.
(40) Coomber, J. W.; Pitts, J. N.; Schrock, R. R. *Chem. Commun.* **1968**, 190.
(41) McDowell, C. A.; Sifniades, S. *J. Am. Chem. Soc.* **1962**, *84*, 4606.
(42) *LUTHER* program: adapted from Luther, F. M.; Gelinas, R. J. *Geophys. Res., 81*, 1125, 1976. Isaksen, I. S. A.; Midtbo, K.; Sunde, J.; Crutzen, P. J. Institut Report Series, No. 20, Institut for geophysic, University of Oslo, 1976.
(43) Gierczak, T.; Burkholder, J. B.; Talukdar, R. K.; Mellouki, A.; Barone, S. B.; Ravishankara, A. R. *J. Photochem. Photobiol.* **1997**, *110*, 1−10.
(44) Grosjean, D.; Grosjean, E.; Williams, E. L., II. *Int. J. Chem. Kinet.* **1993**, *25*, 783−794.
(45) Hein, R.; Crutzen, P. J.; Heimann, M. *Glob. Biogeochem. Cyc.* **1997**, *11*, 43−76.
(46) Meylan, W. M.; Howard, P. H. *Environ. Toxicol. Chem.* **1991**, *10*, 1283−1291.